International Refereed Journal of Engineering and Science (IRJES)
ISSN (Online) 2319-183X, (Print) 2319-1821
Volume 15, Issue 4 (Jul. – Aug. 2026), PP. 107-117

Hydrogeochemical Characteristics of Hot Springs in the Çesme Geothermal Area (İzmir-Türkiye)

Özkan ATEŞ*, Süha ÖZDEN**, Seray ÇINAR YILDIZ***
** (Assistant Professor, Department of Mining and Mineral Extraction, Çan Vocational School, Çanakkale Onsekiz Mart University Çan-Çanakkale, Türkiye)*
*** (Professor, Department of Geological Engineering, Engineering Faculty, Çanakkale Onsekiz Mart University, Çanakkale, Türkiye)*
**** (PhD Student, Department of Geological Engineering, School of Graduate Studies, Çanakkale Onsekiz Mart University, Çanakkale, Turkey)*
Corresponding Author: ozkanates@comu.edu.tr

Abstract: *Karaburun Peninsula is located in Western Anatolia, in the western part of İzmir province. The region is also very rich in terms of geothermal systems. A large part of the existence of these geothermal systems in the region depends on the presence of active faults in the area. When evaluated in terms of earthquakes in the instrumental period, the region is under earthquake risk today as it was in the past. The active tectonic elements on which the geothermal areas in the region are located are the Çeşme and Mordoğan Fault, Gülbahçe Fault Zone, Seferihisar Fault, Tuzla Fault, which extends approximately N-S from west to east, and the İzmir Fault, which extends approximately E-W. Many geothermal areas in İzmir and its surrounding region, which is also very rich in terms of geothermal systems -Balçova, Seferihisar (Cumalı, Doğanbey, Karakoç, Doğanbey Burnu), Çeşme (Ilıca, Şifne), Dikili-Bergama (Kaynarca, Dikili, Nebiler, Bademli, Kocaoba, Paşa, Güzellik), Aliağa (Ilıcaburun, Çukurova, Samurlu, Reşadiye), Bayındır, Urla (Gülbahçe). Most of these geothermal areas are located on active fault zones. Within the scope of this project, on-site measurement and water sampling were carried out in different periods from the hot springs determined in the Ilıca (YLD-BR) and Şifne (SF-N) geothermal areas in the Çeşme district of the Karaburun Peninsula, taking into account seasonal changes, and the hydrogeochemical characteristics of the area were revealed. In addition, in these geothermal areas, suitable Si, Na-K, Na-K-Ca, Mg-Li, Na-Li geothermometers were applied to determine the reservoir temperatures.*

Keywords*: İzmir, Karaburun Peninsula, Geothermal Energy, Hydrogeochemistry*

Date of Submission: 05-08-2026 Date of acceptance: 17-08-2026

I. INTRODUCTION

Geothermal energy is a domestic, renewable, environmentally friendly, locally utilized, sustainable energy source that provides employment and contributes to the local economy. Turkey has an important geological location between Asia and Europe, situated on the tectonically active Alpine-Himalayan Mountain Belt. Therefore, it contains geologically young and active faults, as well as volcanic and magmatic formations. These structures have led to the formation of a rich geothermal potential in Turkey. There are approximately 1000 natural geothermal sources with varying temperatures spread throughout the country [1].

Water, as it passes through its environment, comes into contact with rocks, dissolving and carrying away certain substances. The concentrations of dissolved substances in geothermal fluids, which consist of hot water, steam, and gases, vary depending on the water-rock interaction, duration, and ambient temperature. The movement of geothermal fluid in a geothermal field, its type, origin, age, maximum reservoir rock temperature, recharge height, and mixing ratios with other waters can be explained by water chemistry [2]. Geothermal waters have a high amount of dissolved chemical substances. The solubility of elements depends on the water-mineral balance and is mostly in mineral form. The amounts of elements are a characteristic feature of the temperature and the environment in which they are located. Water chemistry data can be used to explain the temperature, recharge and discharge zones, and mixing ratios with other waters of geothermal systems [3-4].

Geothermometers are one of the most important methods used to determine the reservoir temperature of geothermal waters. Geothermometer equations utilize the chemical composition acquired by the thermal water through interaction with the reservoir rock. Determining the possible reservoir temperature is crucial for the economic operation and development of thermal water. Although there are many types of geothermometers (cation, silica, gas, isotope, etc.), cation and silica geothermometers are generally preferred for estimating reservoir temperature due to their ease of sampling, analysis, and evaluation [5].

The study area, which includes the Tuzla Fault, Seferihisar Fault, Mordoğan Fault and Gülbahçe Fault Zone and its surroundings, which are shown as active faults on the Active Fault Map of Turkey, is located within the province of İzmir (Western Anatolia) (Figure 1).

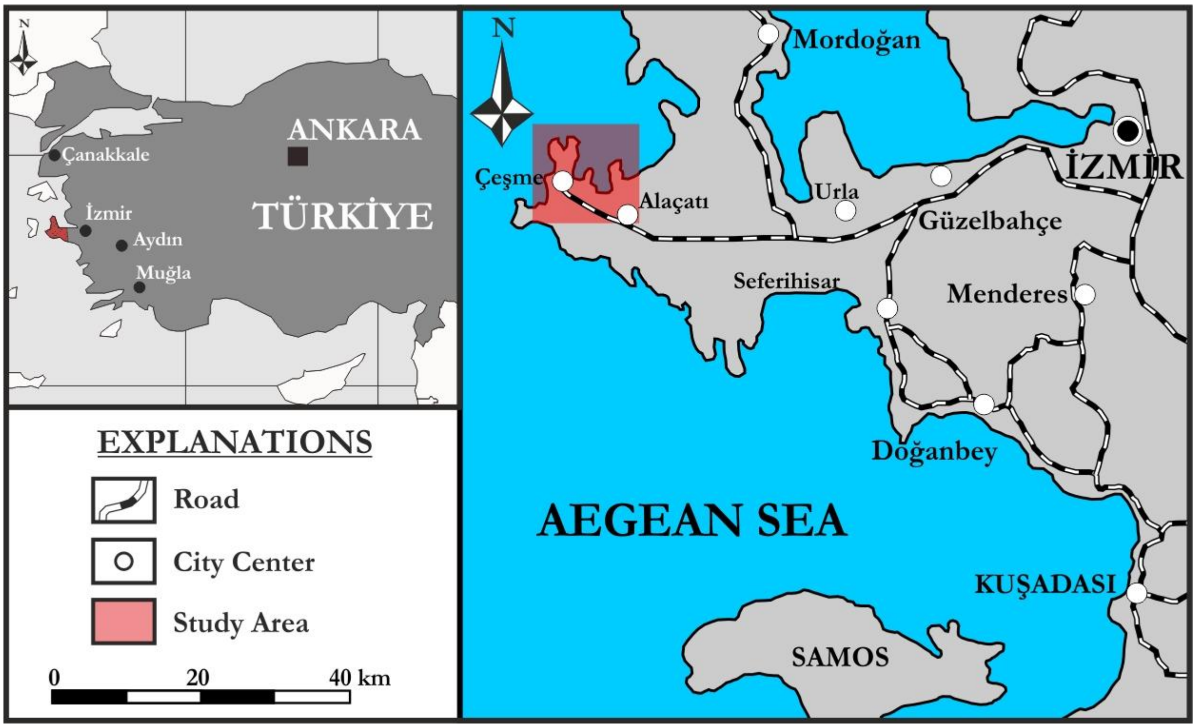

Figure 1. Geographic map of the study area

This study investigated the hydrogeochemical properties of thermal waters in two hot springs located in the Çeşme district of İzmir province, on the Karaburun Peninsula in Western Anatolia. In-situ measurements and hydrogeochemical analyses of hot water samples were conducted at these sources. Sampling and in-situ measurements were performed regularly at specific intervals. The hydrogeochemical characteristics of the thermal waters were determined through in-situ measurements at the source and laboratory hydrogeochemical analyses of the collected hot water samples. This study revealed the hydrogeochemical characteristics of hot springs located in and around Çeşme (İzmir).

II. MATERIALS and METHOD

This study identified hot springs associated with active fault lines in the geothermal area of Çeşme district, İzmir province. These springs are the Şifne and Yıldızburnu hot springs. Regular periodic monitoring was conducted on these two hot springs between May 2023 and March 2024. Measurements of pH, conductivity (EC), temperature (T), total dissolved solids (TDS), and salinity (NaCl) were taken at each spring. Furthermore, major and minor ion (Na, Ca, Mg, Cl, SO_4, HCO_3, Li, B, SiO_2, NH_4, Br, F, PO_4, NO_3 and NO_2) analyses of water samples taken from these hot springs were performed at the GEMAR Environmental Measurement and Analysis Occupational Health and Safety Geology Mining Construction Industry and Trade Ltd. Company, Environmental Measurement and Analysis Laboratory, Çanakkale.

III. CASE STUDY: GEOLOGY AND TECTONICS OF THE STUDY AREA

The Karaburun Peninsula and its immediate surroundings contain rock formations of various ages and types, formed from the Precambrian period (542 million years ago) to the present day.

The basement under the Neogene rock units are composed of carbonate rocks of the Late Triassic, which forms N-S extending structural highlands in the Early Miocene basin in the study area [6]. The lacustrine deposits of the Early-Middle Miocene Çeşme group overlap on these structural uplifts with time-lapse transgressive contacts represented by basal conglomerate levels. The basement rocks cropped out in the eastern part of the peninsula (between Ildır, Ilıca and Germiyan districts) are represented by marine sediments deposited from Silurian to Jurassic. Silurian-Carboniferous turbiditic rocks [7] and Bashkirian-Viseen aged rocks [6] consisting of clastic and carbonate rocks represent the Paleozoic marine deposition. At the bottom of the Mesozoic sequence, which overlies the Paleozoic basement with an angular unconformity, begins with the Scythian transgressive deposits in its lower part and continues with the carbonate rockdominated deep sea sediments during the Anisian [6]. The Camiboğazı formation [8], which reflects the neritic carbonate deposition of the Ladinian period, transitionally overlies the Gerence formation. The Mesozoic deposition continued with shallow marine carbonate rocks in the Upper Triassic (Carnian-Rhaethian), and neritic carbonates were deposited in the Jurassic [7-8].

The Neogene rock units exposed in the Çeşme Peninsula consist of terrestrial deposits and calcalkaline volcanics. The oldest deposits in the study area are represented by lacustrine dominant Çeşme group. Armağandağı volcanics have lateral interfingering contact relationship with the section of the Çeşme group over the Şifne formation (Ovacık formation, Çiftlik formation and Ildır formation [9]), which is the equivalent the last unit]. The Kaştepe group, which overlies all these units with an angular unconformity, has deposits grades from alluvial fan to lacustrine types (Figure 2) [10].

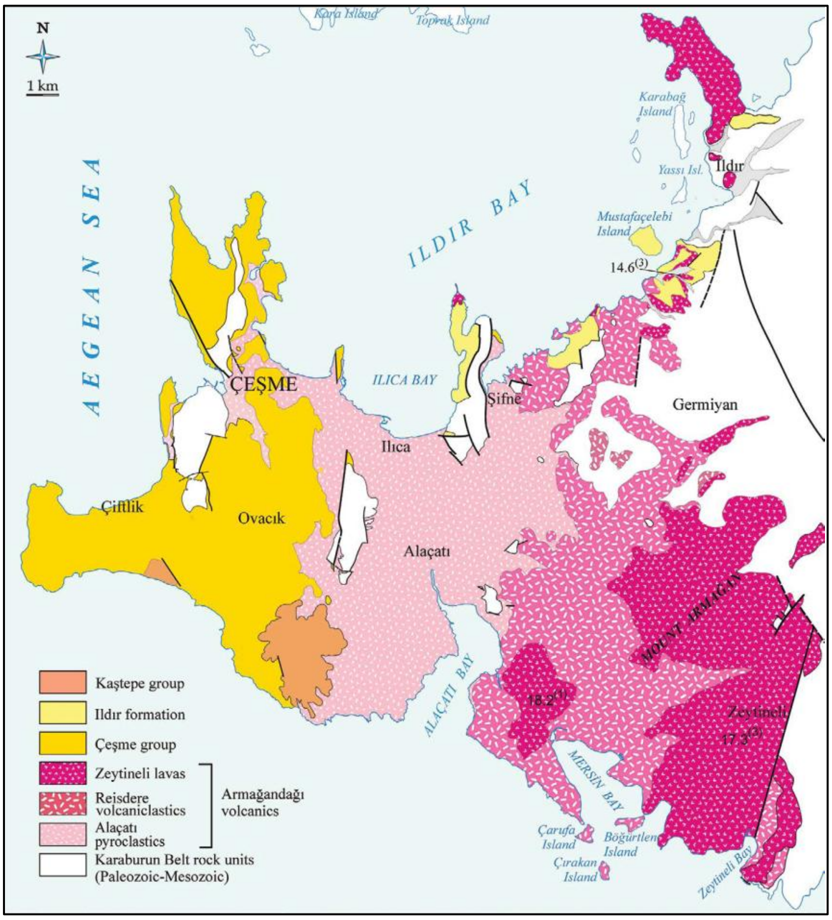

Figure 2. Geological map of the study area and vicinity [11]

The Çeşme geothermal system was formed by seawater seeping underground through fractures, cracks, and karst cavities, where it surfaced due to geothermal gradients, volcanism, and especially along N-S trending fault segments [12]. Deformation in the bedrock around the geothermal field has not reached extreme levels. Neogene volcanosedimentary units have also formed local folds in the areas where they have faulted. The most important structural controls in the Çeşme geothermal field are the N-S trending fault segments. Local subsidence zones have formed around these faults, and these faults extend between Ilıca-Şifne and Alaçatı Bay, dividing the Çeşme Peninsula into different tectonic blocks. Around Alaçatı, there are normal faults extending in a N-S direction that limit the Karadağ uplift south of Ilıca Beach (Figure 3).

The area acquired a significant portion of its present-day morphology through major tectonic lines and associated movements that developed during the Miocene period [13]. Normal faults extending approximately north-south along the slopes of the limestone uplands of the Güvercinlik Formation form contacts with Neogene volcano-sedimentary units. In and around Ilıca, it is estimated that Quaternary and Neogene units cover the faults extending along Karadağ. The north-south trending fault present on the Ilıca coast is located in the continuation of buried faults. This fault, also called the Ilıca Fault, can be considered the most important fault segment providing fluid recharge to the geothermal system by conveying seawater to deeper reservoir levels [13].

Figure 3. Tectonic map of the study area and its immediate surroundings [14, modified from 7]

IV. RESULTS: HYDROGEOCHEMICAL CHARACTERISTICS OF THE STUDY AREA

In this study, in-situ measurements and water sampling were carried out between May 2023 and March 2024 from the hot springs identified in the Ilıca (YLD-BR) and Şifne (SF-N) geothermal areas in Çeşme district, located on the Karaburun Peninsula in İzmir province in Western Anatolia, taking seasonal variations into account, in order to determine the hydrogeochemical characteristics of the area (Figure 4). In addition, suitable Si, Na-K, Na-K-Ca, Mg-Li, and Na-Li geothermometers were applied in these geothermal areas to determine the reservoir temperatures.

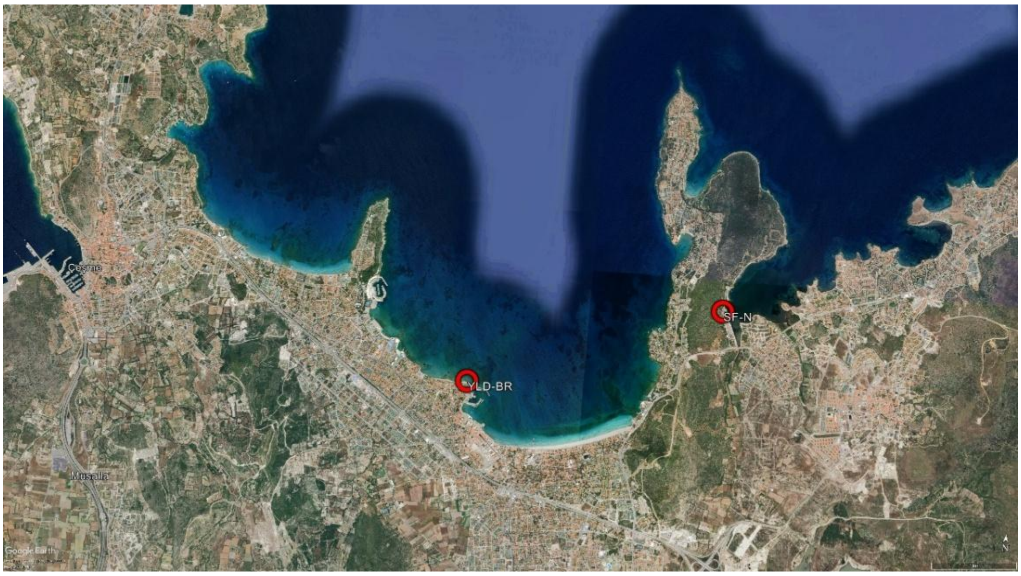

Figure 4. Location of hot springs in the study area

4.1. Yıldızburnu (Çeşme) Hot Spring (YLD-BR)

Located in the west of İzmir province and east of Çeşme district, the Yıldızburnu (YLD-BR) hot spring in the Ilıca Geothermal Area emerges as a natural resource near the sea (Figure 5). In-situ measurements and water sampling studies were conducted in this area during two different periods. In-situ measurements included temperature (T-°C), pH, conductivity (EC-µs), salinity (NaCl), and total dissolved solids (TDS) of the hot spring

(Table 1). Hydrochemical analyses (Na, K, Ca, Mg, Cl, SO_4, HCO_3, Li, B, SiO_2, NH_4, Br, F, PO_4, NO_3, NO_2) were performed on the collected hot water samples. These analyses determined the major and minor ion concentrations of the water.

Ions such as Na, Ca, Mg, K, Cl, HCO_3 and SO_4, which constitute more than 90% of the total ionic content of natural waters, are called major ions. According to the chemical analysis results of the YLD-BR hot spring, the major ion concentrations are presented in Table 2, and the minor ion concentrations are presented in Table 3.

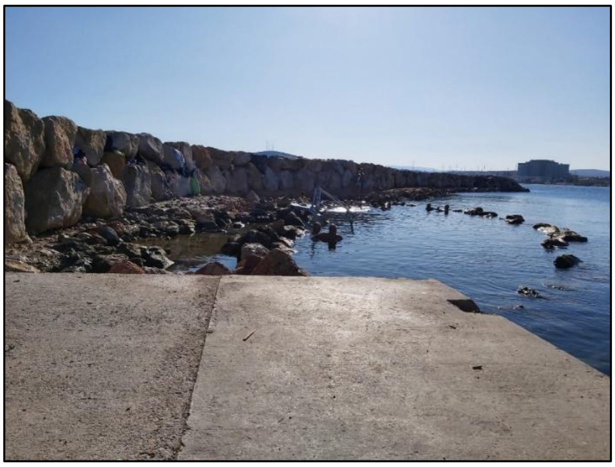

Figure 5. YLD-BR hot spring

Table 1. On-site measurement results of the YLD-BR hot spring

Location	Date	T (°C)	pH	EC (µS/cm)	Salinity (ppm)	TDS (ppm)
YLD-BR	May 2023	39.30	7.01	48600	32600	24300
	March 2024	37.30	6.91	50700	34300	25300

Table 2. Major ion concentrations of the YLD-BR hot spring

Location	Date	Na (mg/l)	K (mg/l)	Ca (mg/l)	Mg (mg/l)	Cl (mg/l)	SO_4 (mg/l)	HCO_3 (mg/l)
YLD-BR	May 2023	18801.50	856.50	1263.02	1991.20	21605.64	3150.98	86.20
	March 2024	21304.30	820.96	1315.37	1801.36	22938.00	3925.16	121.80

Table 3. Minor ion concentrations of the YLD-BR hot spring

Location	Date	Li (mg/l)	B (mg/l)	SiO_2 mg/l)	NH_4 (mg/l)	Br (mg/l)	F (mg/l)	PO_4 (mg/l)	NO_3 (mg/l)	NO_2 (mg/l)
YLD-BR	May 2023	0.52	0.39	0.43	<0.01	64.40	0.76	<0.01	2.76	<0.05
	March 2024	0.29	2.31	<1	0.08	87.40	1.22	<0.1	14.34	120.19

The results of the major anion/cation analyses were plotted on Piper [15] and Schoeller [16] numerical diagrams for hydrogeochemical evaluation to determine the water type. When the water types in the area were examined, the YLD-BR hot spring reflected the Na-Cl water type (Figure 6).

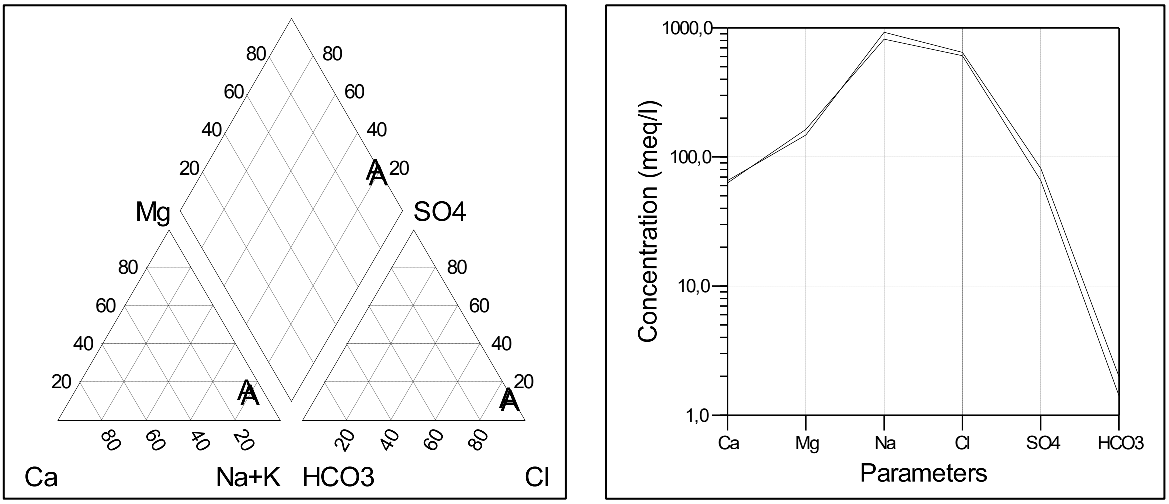

Figure 6. Piper and Schoeller diagrams prepared based on data from the YLD-BR hot spring

Based on the relative abundances of Na, K and Mg in hydrothermal waters, [17] classified the waters into three groups: "immature waters", "partly equilibrated or mixed waters", and "fully equilibrated waters". The term fully equilibrated waters refer to waters that are in equilibrium with respect to all of these components. For this purpose, when the data from hot water samples taken from the YLD-BR hot spring in the study area are plotted on the Na-K-Mg triangular diagram, these waters are classified as partly equilibrated or mixed waters (Figure 7).

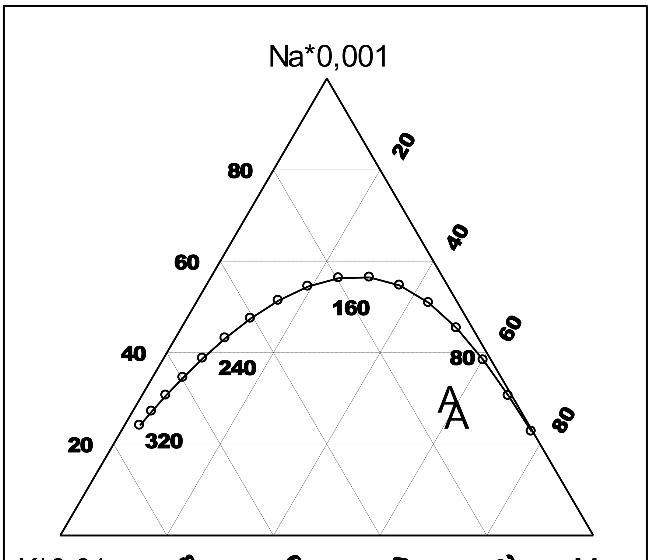

Figure 7. Na-K-Mg diagram of samples taken from the YLD-BR hot spring

By plotting the samples from the YLD-BR hot spring on a Durov diagram [18], it is understood that the main anion is Cl and the cation is Na+K (Figure 8).

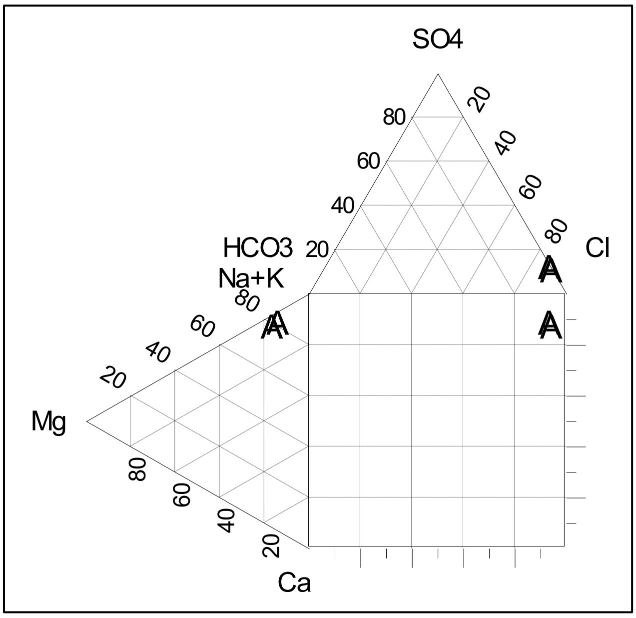

Figure 8. Durov diagram of samples taken from the YLD-BR hot spring

4.2. Şifne (Çeşme) Hot Spring (SF-N)

Located in the west of İzmir province, east of Çeşme district, the Şifne (SF-N) hot spring, situated in the Şifne Geothermal Area, emerges as a natural resource and is used in a hotel operation (Figure 9). In-situ measurement and sampling studies were conducted in this area during five different periods. In the in-situ measurement studies, the temperature (T-°C), pH, conductivity (EC-µs), salinity (NaCl), and total dissolved solids (TDS) of the hot spring were measured (Table 4). Hydrochemical analyses (Na, K, Ca, Mg, Cl, SO_4, HCO_3, Li, B, SiO_2, NH_4, Br, F, PO_4, NO_3, NO_2) were performed on the hot water samples taken. As a result of these analyses, the major and minor ion concentrations of the waters were determined.

Ions such as Na, Ca, Mg, K, Cl, HCO_3 and SO_4, which constitute more than 90% of the total ionic content of natural waters, are called major ions. According to the chemical analysis results of the SF-N hot spring, the major ion concentrations are presented in Table 5, and the minor ion concentrations are presented in Table 6.

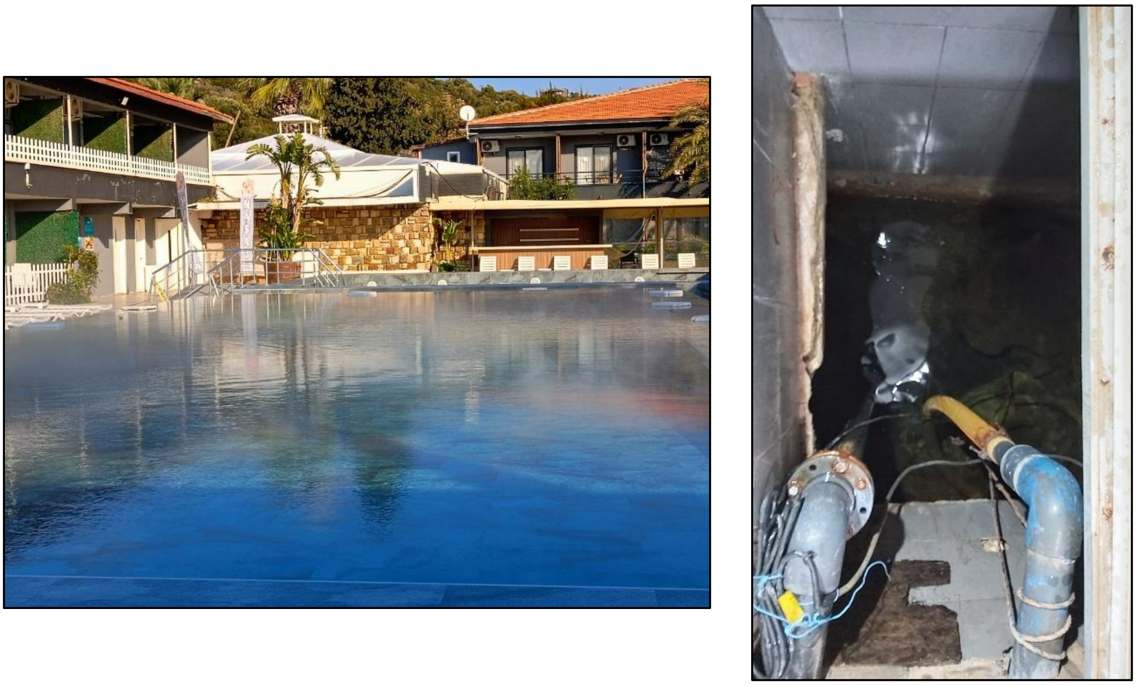

Figure 9. SF-N hot spring

Table 4. On-site measurement results of the SF-N hot spring

Location	Date	T (°C)	pH	EC (µS/cm)	Salinity (ppm)	TDS (ppm)
SF-N	July 2023	40.70	7.22	30700	19600	15400
	August 2023	42.40	7.11	42400	28200	21200
	December 2023	39.10	6.40	45000	30200	22500
	February 2024	39.10	6.80	40900	27100	20500
	March 2024	38.00	6.79	27400	17300	13800

Table 5. Major ion concentrations of SF-N hot spring

Location	Date	Na (mg/l)	K (mg/l)	Ca (mg/l)	Mg (mg/l)	Cl (mg/l)	SO_4 (mg/l)	HCO_3 (mg/l)
SF-N	July 2023	8051.10	864.54	764.80	608.33	17703.38	2411.92	157.00
	August 2023	8758.76	1209.20	649.64	1992.63	17749.36	2458.72	159.60
	December 2023	9729.20	1087.67	714.65	540.92	19937.96	2847.54	167.40
	February 2024	9259.23	908.03	965.56	775.04	15527.24	2138.46	176.20
	March 2024	8029.80	548.30	750.91	685.61	10224.07	1759.00	194.60

Table 6. Minor ion concentrations of SF-N hot spring

Location	Date	Li (mg/l)	B (mg/l)	SiO_2 (mg/l)	NH_4 (mg/l)	Br (mg/l)	F (mg/l)	PO_4 (mg/l)	NO_3 (mg/l)	NO_2 (mg/l)
SF-N	July 2023	0.81	1.23	<1	0.03	51.70	1.30	<0.01	2.54	4.48
	August 2023	0.54	0.49	0.39	0.05	51.06	1.10	<0.01	<0.1	2.66
	December 2023	0.75	0.62	3.21	0.12	60.06	1.14	<0,1	1.13	7.40
	February 2024	2.90	2.23	0.39	0.03	44.44	1.02	<0.1	<0.1	5.32
	March 2024	0.21	0.96	1.93	0.02	33.28	0.79	<0.1	5.83	45.06

The results of the major anion/cation analyses were plotted on Piper [15] and Schoeller [16] numerical diagrams for hydrogeochemical evaluation to determine the water type. When the water types in the area were examined, the SF-N hot spring reflected the Na-Mg-Cl and Na-Cl water type (Figure 10).

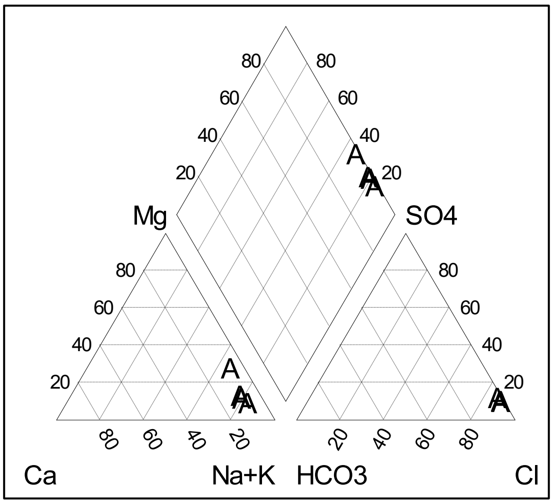

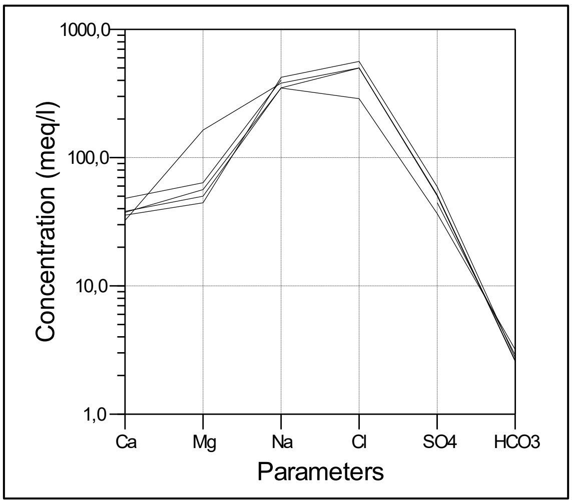

Figure 10. Piper and Schoeller diagrams prepared based on data from the SF-N hot spring

Based on the relative abundances of Na, K and Mg in hydrothermal waters, [17] classified the waters into three groups: “immature waters”, “partly equilibrated or mixed waters”, and “fully equilibrated waters”. The term fully equilibrated waters refer to waters that are in equilibrium with respect to all of these components. For this purpose, when the data from hot water samples taken from the SF-N hot spring in the study area are plotted on the Na-K-Mg triangular diagram, these waters are classified as partly equilibrated or mixed waters (Figure 11).

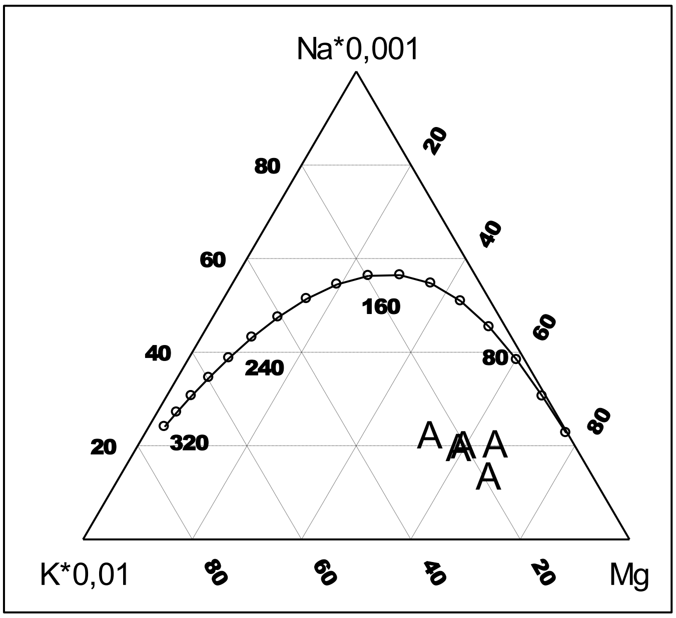

Figure 11. Na-K-Mg diagram of samples taken from SF-N hot spring

By plotting the samples from the SF-N hot spring on a Durov diagram [18], it is understood that the main anion is Cl and the cation is Na+K+Mg (Figure 12).

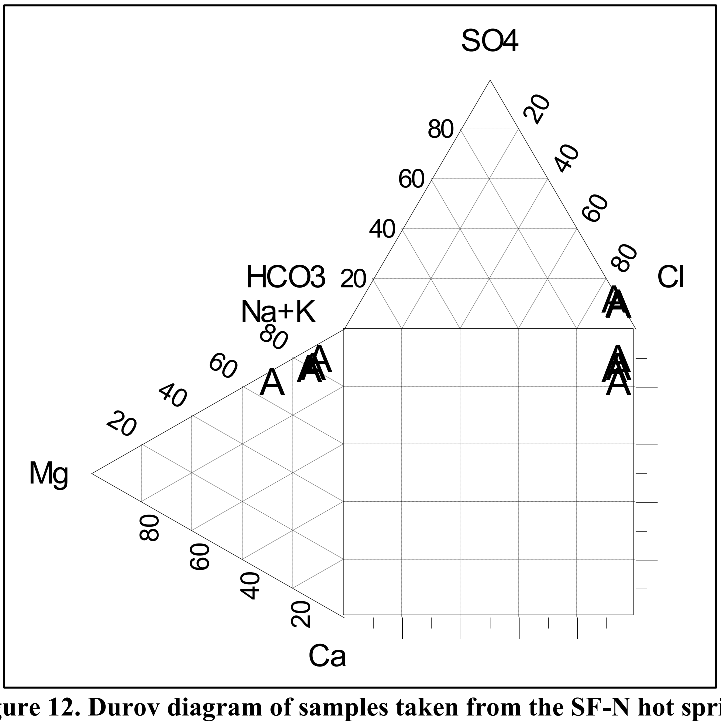

Figure 12. Durov diagram of samples taken from the SF-N hot spring

4.3. Geothermometer Calculations

The general purpose of geothermometers is to estimate the temperature of the underground fluid (i.e., the aquifer temperature or reservoir temperature of the water). As is known, hot waters have very different uses depending on their surface temperature. Hot waters in reservoirs deep underground cool down considerably and mix with cold groundwater in varying proportions before reaching the surface. It is clear that the temperature of the fluid deep underground will be much higher than its surface temperature. Drilling deep underground requires considerable cost and time. Therefore, estimating the temperatures in the reservoir using various geothermometer methods before deep drilling to determine the uses of the water constitutes an important part of geothermal research [19].

The geothermal calculations used to determine reservoir temperatures generally utilize silica and cation geothermometers (Table 7). However, since chemical analyses of hot water samples from both hot springs in the study area revealed low SiO_2 ion concentrations in both sources, silica geothermometers were not considered because they yielded values very close to or lower than the surface temperature of the source. In this study, only cation geothermometers were used for both sources (Table 8).

Table 7. Cation geothermometer equations (concentrations in ppm)

No	Geothermometer	Jeotermometre Equation (t= °C)	Temperature Range (°C)	Reference
1	Na-K	t°C =(856/(0.857+log(Na/K)))-273.15	100-275	[20]
2	Na-K	t°C =(833/(0.780+log(Na/K)))-273.15		[21]
3	Na-K	t°C =(933/(0.993+log(Na/K)))-273.15	25-250	[22]
4	Na-K	t°C =(1319/(1.699+log(Na/K)))-273.15	250-350	[22]
5	Na-K	t°C =(1217/(1.483+log(Na/K)))-273.15		[23]
6	Na-K	t°C =(1178/(1.470+log(Na/K)))-273.15		[24]
7	Na-K	t°C =(1390/(1.750+log(Na/K)))-273.15		[17]
8	K-Mg	t°C =(2330/(7.35-log(K^2/Mg)))-273.15		[25]
9	K-Mg	t°C =(4410/(14-log(K^2/Mg)))-273.15		[17]
10	Li-Mg	t°C =(2200/(5.47-log(Li/$Mg^{0.5}$)))-273.15		[26]

Table 8. Reservoir temperatures calculated using cation geothermometers (°C)

Location	Date	Equation									
		1	2	3	4	5	6	7	8	9	10*
YLD-BR	May 2023	116	120	137	161	158	146	176	214	113	24
	March 2024	104	106	124	151	147	135	166	215	113	15
SF-N	July 2023	196	203	217	221	223	210	238	274	131	43
	August 2023	225	235	247	242	246	232	259	246	123	25
	December 2023	200	208	222	224	227	213	241	308	141	43
	February 2024	186	193	207	214	215	202	231	266	129	68
	March 2024	150	155	171	187	186	174	204	222	115	18

* Below or very close to the surface temperature

V. CONCLUDING REMARKS

In this study, in-situ measurements and water sampling were carried out periodically between May 2023 and March 2024 from two separate hot springs identified in the geothermal fields of Çeşme district, located on the Karaburun Peninsula in western İzmir province, Western Anatolia. These fields are the Ilıca and Şifne geothermal fields in Çeşme district of İzmir province. The hot spring in the Ilıca geothermal field was named YLD-BR and the hot spring in the Şifne geothermal field was named SF-N. The physical and chemical parameters of the hot springs were determined, and their hydrogeochemical properties were revealed.

According to in-situ measurements made at the YLD-BR and SF-N hot springs, the temperatures of the hot springs were determined to be between 37.30-39.30 °C and 38.00-42.40 °C, respectively, and their electrical conductivity was determined to be between 48600-50700 µS/cm and 27400-45000 µS/cm, respectively.

Hydrogeochemical analyses revealed that the water types identified reflect Na-Cl for the YLD-BR hot spring and Na-Cl and Na-Mg-Cl for the SF-N hot spring.

Analysis of samples from the YLD-BR hot spring determined that the main anion is Cl and the cation is Na+K. Analysis of samples from the SF-N hot spring determined that the main anion is Cl and the cation is Na+K+Mg.

When the data from hot water samples taken from YLD-BR and SF-N sources in the study area were plotted on a Na-K-Mg triangular diagram, it was determined that these waters belong to the partly equilibrated or mixed waters class.

According to the results of geothermometer calculations performed to determine the reservoir temperature in the hot springs, the reservoir temperatures were calculated to be between 113-215 °C for the YLD-BR hot spring and between 115-308 °C for the SF-N hot spring.

ACKNOWLEDGEMENT

This study was conducted within the scope of ÇOMÜ-BAP-FHD-2023-4405 project of the Scientific Research Projects Coordination Unit of Çanakkale Onsekiz Mart University. We would like to thank the ÇOMÜ-BAP Coordination Unit for their financial support.

REFERENCES

[1]. Dağıstan, H., 2022. Türkiye Jeotermal Kaynak Aramaları, Kullanımı ve Sürdürülebilirliğinin Sağlanması, MTA Doğal Kaynaklar ve Ekonomi Bülteni, MTA Genel Müdürlüğü.
[2]. Eroğlu, A. ve Aksoy, N., 2005. Jeotermal Suların Kimyasal Analizi, Jeotermal Enerji Semineri, TMMOB Makina Mühendisleri Odası, İzmir, Kasım 2005.
[3]. Ellis, A. J., 1979. Chemical geothemometry in geothermal systems, Geothermics, 25, 219-226.
[4]. Yıldırım, N., 1999. Uygulamalı Jeokimya-2000 li yıllarda jeotermal enerji yaz okulu ders notları, Dokuz Eylül Üniversitesi, İzmir.
[5]. Doğdu, M. Ş., 2004. Jeotermal Suların Rezervuar Sıcaklığının Tahmininde Kullanılan Jeotermometre Hesaplamaları İçin Bilgisayar Programı, Jeoloji Mühendisliği Dergisi, 28 (2), 1-12.
[6]. Erdoğan, B., Altıner, D., Güngör, T., Özer, S., 1990. Stratigraphy of Karaburun Peninsula, Bulletin of the Mineral Research and Exploration, 111, 1-20.
[7]. Çakmakoğlu, A., and Bilgin, R., 2006. Karaburun Yarımadasının Neojen Öncesi Stratigrafisi, Maden Tetkik ve Arama Dergisi, 132:33-62.
[8]. Brinkmann, R., Flügel, E., Jacopshagen, V., Lechner, H., Rendel, B., Trick, P., 1972. Trias, Jura und Unterkreide der Halbinsel Karaburun (West Anatolien). Geologie et Paleontologie, 6, 139-150.
[9]. Göktaş F., 2016. Ildır Körfezi güneyindeki bölgenin Neojen stratigrafisi, Çeşme Yarımadası (Batı Anadolu), Türkiye Jeoloji Bülteni 59:3:299-321.
[10]. Göktaş, F., 2020. Neogene stratigraphy and regional correlation of the Çeşme Peninsula, Western Anatolia, Turkey, Bull. Min. Res. Exp., 162, 31-54.
[11]. Göktaş, F., 2010, Çeşme Yarımadası'ndaki Neojen tortullaşması ve volkanizmasının jeolojik etüdü, Maden Tetkik ve Arama Genel Müdürlüğü Rapor No: 11389, 64 s. Ankara (unpublished).
[12]. Koçak, A., 1974. Çeşme Ilıcası Hidrojeoloji Etüd Raporu. MTA Raporu, No.29588, Yayınlanmamış.
[13]. Yücel, M., Taşkıran, A., Üçer, A., Arslan, S., Toker, E., 2002. Çeşme Yarımadası Jeotermal Alanı Jeoloji ve Jeofizik Etüt Raporu, MTA, Ankara.
[14]. Emre, Ö., Özalp, S., Doğan, A., Özaksoy, V., Yıldırım, C. ve Göktaş, F., 2005a. İzmir yakın çevresinin diri fayları ve deprem potansiyelleri. MTA Genel Müdürlüğü Jeoloji Etütleri Dairesi, Rapor No: 10754, 80s., Ankara.
[15]. Piper, A. M., 1944. A Graphic Procedure in the Geochemical Interpretation of Water-Analyses. Eos, Transactions American Geophysical Union, 25, 914-928.
[16]. Schoeller, H., 1955. Geochemie Des Eaux Souterraines, Revue De L'institute Francois Du Petrole, 10, 230-44.
[17]. Giggenbach, W. F., 1988. Geothermal solute equilibria. Derivation of Na-K-Mg-Ca geoindicators, Geochimica et Cosmochimica Acta. 55, 2749-2765.
[18]. Durov, S. A. 1948. Classification of natural waters and graphical representation of their composition. Dokl. Akad. Nauk. USSR. 59(1):87-90.
[19]. Tarcan, G., 2002. Jeotermal Su Kimyası, Jeotermal Enerji Araştırma ve Uygulama Merkezi (Jenarum) Yaz Okulu Ders Notları, İzmir, s. 230-272.
[20]. Truesdell, A. H., 1976, Summary of section III geochemical techniques in exploration. Proc. of Second United Nations Symposium on the Development and Use of Geothermal Resources, 1975, San Francisco, U.S. Gov. Print. Office, pp. 53-79.
[21]. Tonani, F., 1980, Some remarks on the application of geochemical techniques in geothermal exploration. Adv. Eur. Geoth. Res. Second Symp., Strasbourg, pp. 428-443.
[22]. Arnnórsson, S., Gunnlaugsson, E., Svavarsson, H., 1983, The chemistry of geothermal waters in Iceland. III. chemical geothermometry in geothermal investigations. Geochimica et Cosmochimica Acta, 47, 567-577.
[23]. Fournier, R. O., 1979. A revised equation for the Na-K geothermometer. Geothermal Res. Council Trans. 3, 221-224.
[24]. Nieva, D. and Nieva, R., 1987. Developments in Geothermal Energy in Mexico Part 12. A Cationic Composition Geothermometer for Prospecting of Geothermal Resources. Heat Recovery Systems and CHP, 7, 243-258.
[25]. Fournier, R. O., 1991. Water geothermometers applied to geothermal energy. Application of Geochemistry in Geothermal Reservoir Development, D'Amore, F. (coord.), UNITAR/UNDP, Rome. pp. 37-69.
[26]. Kharaka, Y. K., Mariner, R. H., 1989. Chemical geothermometers and their application to formation waters from sedimentary basins. Thermal History of Sedimentary Basins; Methods and Case Histories, N. D. Näser and T. H. McCulloh (eds.), Springer Verlag, pp. 99-117.